PROCEEDINGS OF SCIENCE

QCD plasma instability and thermalisation at heavy ion collisions

Dietrich Bödeker
Fakultät für Physik, Universität Bielefeld, D-33615 Bielefeld, Germany
E-mail: `bodeker@physik.uni-bielefeld.de`

Kari Rummukainen*
Department of Physical Sciences, P.O.Box 3000, 90014 University of Oulu, Finland
E-mail: `kari.rummukainen@oulu.fi`

Under suitable non-equilibrium conditions QCD plasma can develop plasma instabilities, i.e. exponential growth of some modes of the plasma. It has been argued that these instabilities can play a significant role in the thermalisation of the plasma in heavy-ion collision experiments. We study the instability in SU(2) plasmas using the hard thermal loop effective lattice theory, which is suitable for studying real-time evolution of long wavelength modes in the plasma. We observe that under suitable conditions the plasma can indeed develop an instability which can grow to a very large magnitude, necessary for the rapid thermalisation in heavy-ion collisions.

The XXV International Symposium on Lattice Field Theory
July 30-4 August 2007
Regensburg, Germany

*Speaker.

PoS(LATTICE 2007)220

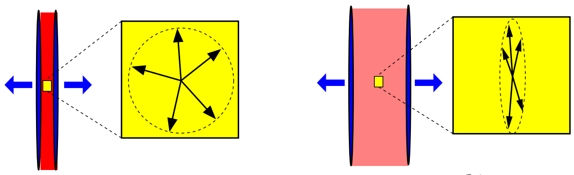

Figure 1: The longitudinal expansion of the collision volume makes the initial parton momentum distribution (a) squeezed along the plane perpendicular to the collision axis (b).

1. Introduction

One of the most striking results from the heavy ion collision experiments at RHIC is the rapid thermalisation of the plasma; the thermalisation appears to occur in time $\lesssim 1\text{fm}/c$ after the collision [1]. At sufficiently large collision energy the QCD coupling is small and perturbation theory should be applicable. However, it turns out that the perturbative processes cannot alone explain rapid thermalisation [2, 3]. It has been argued that the strongly non-equilibrium initial conditions may lead to exponential growth of certain long wavelength modes of the plasma — *plasma instability* [4]. These growing modes might play a significant role in the thermalisation of the plasma. The plasma instability arises because the plasma initially expands predominantly along the collision axis ($\hat{z}$ direction), and the momentum distribution of the produced partons becomes anisotropic: the momentum distribution becomes much smaller along z-axis direction than along the transverse directions, no matter what the initial distribution of the partons was (Fig. 1). The initial momenta of the partons is of order of $\sim$ few GeV (which is the saturation scale of the original nuclei in color glass condensate models), which we denote as the “hard” scale.

The hard partons will interact with the soft gauge fields; assuming that the soft fields have small initial amplitude the non-abelian nature of the fields can be ignored. In this case the anisotropic parton momentum distribution causes the soft fields to become unstable against the generation of $\hat{x}$ and $\hat{y}$ -direction magnetic fields: the magnetic fields focus the current carried by the partons by amplifying the inhomgeneities in it, which in turn leads to increasing magnetic fields. This leads to exponential increase in the magnitude of the magnetic fields, analogously to the Weibel instability in electromagnetic plasmas (Fig. 2). However, for the case of QCD the current is mostly carried by saturation scale partons, which are mostly hard gluons.

The growth in the small-field regime happens only in a certain range of wave vectors (depending on the degree of anisotropy in the hard parton distribution) and it is maximal at a particular wave vector, $\boldsymbol{k}_*$, oriented along $\hat{z}$-direction. In QED the growth can continue until the magnitude of the gauge field reaches $eA \sim p_{\text{hard}}$; when this happens the hard charged particles are deflected to random directions and their distribution becomes isotropic. However, in QCD the field equations become non-linear at much smaller magnitude $gA_{k_*} \sim k_*$ (or $B^2 \sim g^2 k_*^4$), because $k_* \ll p_{\text{hard}}$. Thus, the central question is what happens to the unstable growth when the magnitude of the chromomagnetic fields reaches this “non-abelian” value. In Ref. [5] it was suggested that the growth could persist beyond the non-abelian value if the system “abelianises,” i.e. it becomes essentially dominated by only one color degree of freedom. Thus, as the fields continue growing the distribution can isotropize through the mechanism described above.

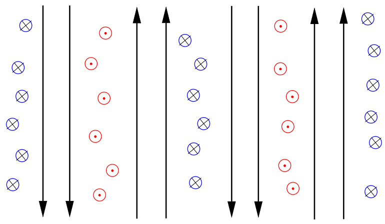

Figure 2: The Weibel instability in the electromagnetic plasma. Arrows show the electric current, circles the magnetic flux perpendicular to the plane. The magnetic field amplifies the inhomogeneities in the current, which in turn amplifies the magnetic fields.

Because of the large amplitude of the chrmomagnetic fields the problem is non-linear and non-perturbative. The cleanest way to approach the problem is to perform real-time evolution on the lattice using so-called "hard loop approximation": the infrared modes are classical chromomagnetic fields, and the hard partons are treated as a classical charged particle current on the soft field background. This approximation is justified because we will be dealing with large occupation numbers for the soft fields, and the expansion renders the hard particle distribution dilute. We also consider only non-expanding systems with fixed anisotropic hard particle momentum distributions in order to focus on the effects of the anisotropy. Physically this corresponds to sufficiently large times where the expansion rate is parametrically small compared to the rates associated with the instability.

This approach has previously been applied to 1+1 -dimensional case [6] where it was observed that the fields indeed continue to grow in the non-linear regime. However, 3+1 dimensional simulations with moderate anisotropies have indicated that the instabilities are quenched as the non-linearities become important [7, 8]. In this work we shall study considerably stronger momentum anisotropies than above, together with large lattice volumes and small lattice spacing. A detailed report of the results can be found in [9]. Strong anisotropies are also studied in Ref. [10], but with initial conditions not leading to further exponential growth.

2. Hard Loop effective theory

The hard modes are described as on-shell particles moving in soft background fields, with a distribution function

$$f_{\rm hard}(x,\boldsymbol{p}) = \bar{f}(\boldsymbol{p}) + \lambda^a f^a(x,\boldsymbol{p}) + \ldots \qquad (2.1)$$

where the anisotropic gauge singlet part $\bar{f}(\boldsymbol{p})$ we assume to be constant in space and time, and f^a describes fluctuations in the current carried by the particles. The system evolves according to the Yang-Mills-Vlasov equations of motion

$$(D_\mu F^{\mu\nu})^a = J^{a,\nu}_{\rm hard} = g\int_{\boldsymbol{p}} v^\nu f^a, \qquad (v\cdot Df)^a + gv^\mu F^a_{\mu i}\frac{\partial \bar{f}}{\partial p^i} = 0, \qquad (2.2)$$

where $v = (1,\boldsymbol{p}/p)$. Defining

$$W^a(x,\boldsymbol{v}) \equiv 4\pi g \int_0^\infty \frac{dp\,p^2}{(2\pi)^3} f^a(x,\boldsymbol{p}) \qquad (2.3)$$

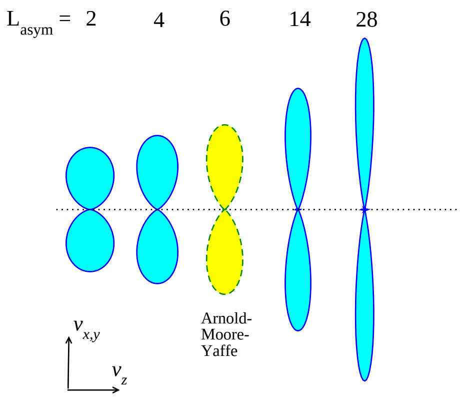

Figure 3: Anisotropic hard particle distributions used in this work, together with the distribution used by Arnold, Moore and Yaffe [7]. The distributions are plotted so that the relative number of particles moving to direction $\boldsymbol{v}$ is proportional to the length of the radial vector from the center of the plot.

we can integrate the equations of motion over $|p|$, obtaining

$$(D_\mu F^{\mu\nu})^a = \int \frac{d\Omega_{\boldsymbol{v}}}{4\pi} v^\nu W^a, \qquad (v\cdot DW)^a = m_0^2 v^\mu F^a_{\mu i} U^i(\boldsymbol{v}). \tag{2.4}$$

Here the vector $U^i(\boldsymbol{v})$ characterises the anisotropic singlet part of the hard distribution $\bar{f}$:

$$m_0^2 U^i(\boldsymbol{v}) = -4\pi g^2 \int_0^\infty \frac{dp p^2}{(2\pi)^3} \frac{\partial \bar{f}(p\boldsymbol{v})}{\partial p^i}. \tag{2.5}$$

For thermal distribution $\bar{f}$ becomes isotropic, and we would obtain $\boldsymbol{U} = \boldsymbol{v}$ and $m_0 = m_{\text{Debye}}$, the Debye mass of the thermal plasma. We note that m_0 is the only dimensionful parameter in the problem.

The equations of motion 2.4 are discretised on the lattice. The current carried by the hard particles is described by the $W^a(x,\boldsymbol{v})$-fields. These are quite expensive to handle, because they live on manifold $R^3 \times S^2$. We treat these by expanding the distributions in spherical harmonics:

$$W^a(x,\boldsymbol{v}) = \sum_{\ell m} W^a_{\ell m} Y_{\ell m}(\boldsymbol{v}), \qquad \bar{f}(\boldsymbol{p}) = \sum_\ell \bar{f}_\ell(p) Y_{\ell 0}(\boldsymbol{v}), \tag{2.6}$$

where $\ell = 0\ldots L_{\max}$, the cut-off in spherical harmonics expansion. Thus, at each site W^a has $(L_{\max}+1)^2$ real degrees of freedom. This approach has been also used in Refs. [7, 10] to study the plasma instablity. Originally, this method was successfully applied to the calculation of the sphaleron rate in hot SU(2) gauge theory on the lattice [11].

For simplicity, we are using SU(2) gauge group in our analysis. We present the results using 4 different values for the anisotropy of the $\bar{f}$, both weaker and much stronger than used in [7]. Each distribution is characterised by the maximal spherical harmonic index used to parametrise $\bar{f}$, $L_{\text{asym}} = 2$, 4, 14 and 28 ($L_{\text{asym}} < L_{\max}$). For each value of L_{asym} we approximately maximised the possible asymmetry of the distribution; the motivation for this is that this choice should minimise the required $L_{\max}$ cutoff. The anisotropic distributions are shown in Fig. 3. The degree of the anisotropy is characterised by the *anisotropy parameter* $\eta^2 \equiv 3\langle v_z^2\rangle/\langle v^2\rangle$; for the distributions here this is $\eta^2 = 0.6$, 0.4, 0.086 and 0.022 for $L_{\text{asym}} = 2$, 4, 14 and 28.

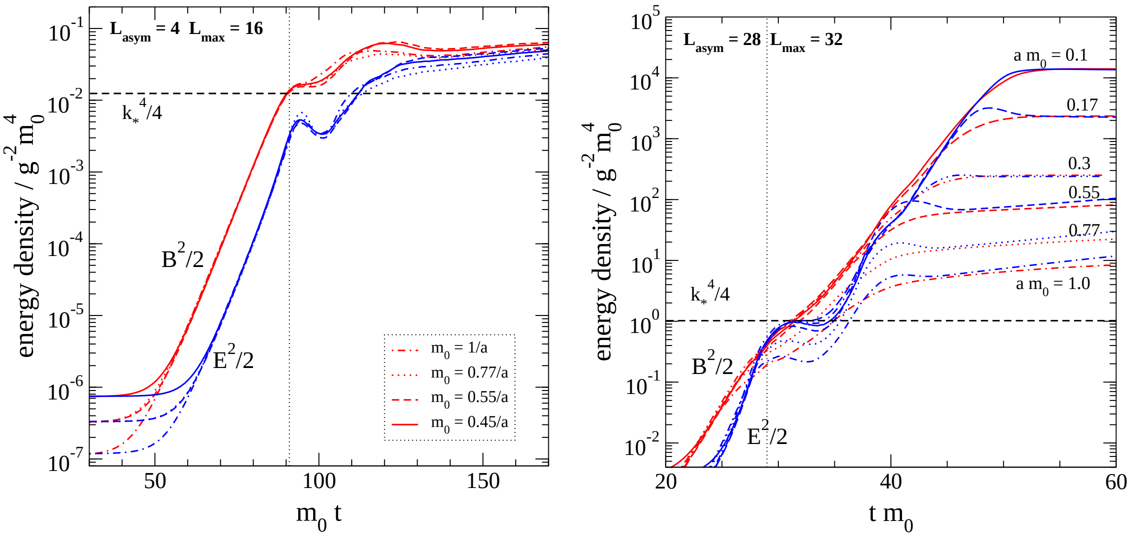

Figure 4: Growth of the energy with small (left) anisotropy, $L_{\rm asym} = 4$ and large (right) anisotropy, $L_{\rm asym} = 28$. In both cases the energy grows until the magnitude of the growing magnetic field reaches the value where non-abelian effects become significant; $B^2 \sim (k^*)^2$. With strong anisotropy, the growth continues until regulated by the lattice cutoff.

In our simulations we are using very large lattice volumes (up to 240^3) and vary the lattice spacing by more than order of magnitude. The $L_{\rm max}$-cutoff is up to 48. In general, the infinite volume and continuum limits are under control; for details, see [9].

3. Results

In Fig. 4 we show the growth of the soft field energy density at small and large anisotropy, measured at different lattice spacings. Initially the soft fields have small white noise fluctuations. In both cases the instability causes exponential growth of energy density in the linear (weak field) region. However, when the field evolution becomes non-linear (shown as vertical lines), the growth is rapidly quenched at weak anisotropy, independent of the lattice spacing. This is in accord with the results of Ref. [7].

However, at strong anisotropy the growth continues in the non-linear regime, and the smaller the lattice spacing is, the further the growth persists. The cutoff is due to lattice cutoff, as can be seen in Fig. 5: here we show the chromomagnetic field energy density at final saturation as a function of the lattice spacing. The saturation energy is well described as a power law of the lattice spacing.

Thus, the results clearly indicate that unstable growth is possible in the non-linear regime. What field modes do grow here? We study this by fixing to Coulomb gauge and measuring the occupation numbers of the gauge field, $f(\boldsymbol{k}) \propto |\boldsymbol{k}|A(\boldsymbol{k})$. The evolution of the occupation numbers at large anisotropy is shown in Fig. 6. In the linear (early) regime the growth near $k_* \approx m_0$ is clearly visible. However, when the system becomes non-linear at $f(k_*) \sim 1$, the growth at k_* is completely quenched, but $f(k)$ at higher wave numbers shoots rapidly up. The final occupation number distribution is very close to the thermal one. Thus, the growth mechanism appears to

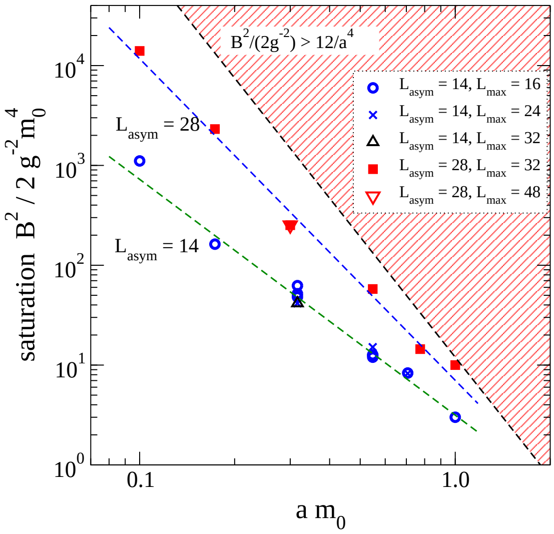

Figure 5: Saturation magnetic field energy as a function of the lattice spacing at large anisotropies. The red hashed area is forbidden because energy density there is too large to be supported by the lattice.

be very different from the abelianisation proposed in [5]. We have checked this behaviour using various gauge invariant measurements (k-sensitive operators, cooling), with fully consistent results, see Ref. [9]. Unstable growth in the non-linear regime has also been observed in Ref. [12], but using very different methodology.

In summary, we observe clear signal of rapid soft field energy growth in the non-linear (large magnitude) regime when the hard particle distribution is strongly anisotropic, suggesting possible role in the thermalisation of the plasma in heavy ion collision experiments. However, the mechanism through which the growth proceeds is still unknown and under further study. There are also important caveats: perhaps most significantly, the initial conditions in the cases reported here all have small magnitude soft fields. When the magnitude of the initial fields is increased the non-linear growth is reduced [9, 10].

DB acknowledges support from DFG funded Graduate School GRK 881, and KR support from Academy of Finland grants 104382 and 114371. The simulations in this work have been performed at the Finnish IT Center for Science (CSC, Espoo, Finland).

References

[1] See the discussion in K. Adcox *et al.* [PHENIX Collaboration], *Formation of dense partonic matter in relativistic nucleus nucleus collisions at RHIC: Experimental evaluation by the PHENIX collaboration*, Nucl. Phys. A **757** (2005) 184 [arXiv:nucl-ex/0410003].

[2] R. Baier, A. H. Mueller, D. Schiff, D. T. Son, *'Bottom-up' thermalization in heavy ion collisions*, Phys. Lett. B **502** (2001) 51 [arXiv:hep-ph/0009237].

[3] D. Bödeker, *The impact of QCD plasma instabilities on bottom-up thermalization*, JHEP **0510** (2005) 092 [arXiv:hep-ph/0508223].

[4] S. Mrowczynski, *Plasma instability at the initial stage of ultrarelativistic heavy ion collisions*, Phys. Lett. B **314** (1993) 118.

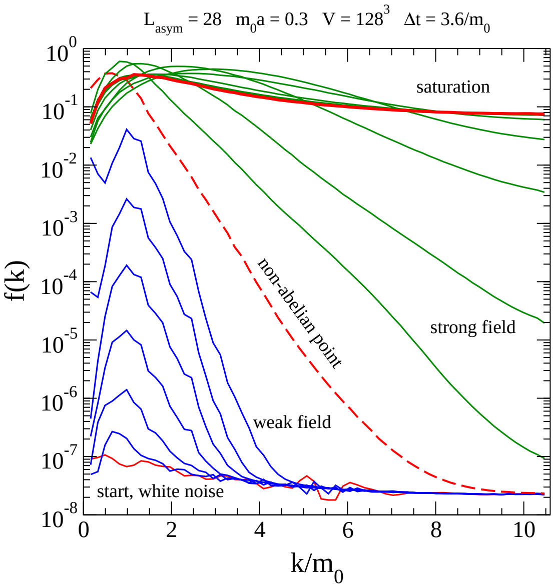

Figure 6: Coulomb gauge power spectrum (occupation number) as a function of time for strong anisotropy. The spectra are plotted at time intervals of $\Delta t = 3.6/m_0$, with the initial state at bottom, and the final state near the top.

[5] P. Arnold and J. Lenaghan, *The abelianization of QCD plasma instabilities*, Phys. Rev. D **70** (2004) 114007 [arXiv:hep-ph/0408052].

[6] A. Rebhan, P. Romatschke and M. Strickland, *Hard-loop dynamics of non-Abelian plasma instabilities*, Phys. Rev. Lett. **94** (2005) 102303 [arXiv:hep-ph/0412016].

[7] P. Arnold, G. D. Moore and L. G. Yaffe, *The fate of non-abelian plasma instabilities in 3+1 dimensions*, Phys. Rev. D **72** (2005) 054003 [arXiv:hep-ph/0505212].

[8] A. Rebhan, P. Romatschke and M. Strickland, *Dynamics of quark-gluon plasma instabilities in discretized hard-loop approximation*, JHEP **0509** (2005) 041 [arXiv:hep-ph/0505261].

[9] D. Bodeker and K. Rummukainen, *Non-abelian plasma instabilities for strong anisotropy*, JHEP **0707** (2007) 022 [arXiv:0705.0180 [hep-ph]].

[10] P. Arnold and G. D. Moore, *Non-Abelian Plasma Instabilities for Extreme Anisotropy*, Phys. Rev. D **76** (2007) 045009 [arXiv:0706.0490 [hep-ph]].

[11] D. Bödeker, G. D. Moore and K. Rummukainen, *Chern-Simons number diffusion and hard thermal loops on the lattice*, Phys. Rev. D **61** (2000) 056003 [arXiv:hep-ph/9907545].

[12] A. Dumitru, Y. Nara and M. Strickland, *Ultraviolet avalanche in anisotropic non-Abelian plasmas*, Phys. Rev. D **75** (2007) 025016 [arXiv:hep-ph/0604149].